NeuroImage: Clinical 23 (2019) 101898

Contents lists available at ScienceDirect

NeuroImage: Clinical

journal homepage: www.elsevier.com/locate/ynicl

Trunk rotation and handedness modulate cortical activation in neglect-associated regions during temporal order judgments

Kerstin Paschke[a,b,d,*], Mathias Bähr[d,e], Torsten Wüstenberg[c,g,1], Melanie Wilke[a,e,f,h,1]

[a] Department of Cognitive Neurology, University Medicine Göttingen, Robert-Koch-Str. 40, Göttingen 37075, Germany
[b] German Center for Addiction Research in Childhood and Adolescence, University Medical Center Hamburg-Eppendorf, Martinistr. 52, Hamburg 20246, Germany
[c] Department of Psychiatry and Psychotherapy, Charité - Universitätsmedizin Berlin, Corporate Member of Freie Universität Berlin, Berlin Institute of Health, Humboldt-Universität zu Berlin, Charité Campus Mitte, Charitéplatz 1, Berlin 10117, Germany
[d] Department of Neurology, University Medicine Göttingen, Robert-Koch-Str. 40, Goettingen 37075, Germany
[e] DFG Center for Nanoscale Microscopy & Molecular Physiology of the Brain (CNMPB), Germany
[f] German Primate Center, Leibniz Institute for Primate Research, Kellnerweg 4, Göttingen 37077, Germany
[g] Systems Neuroscience in Psychiatry (SNiP), Central Institute of Mental Health, Mannheim, J5, Mannheim 68159, Germany
[h] Leibniz-science campus primate cognition, Germany

ARTICLE INFO

Keywords:
Spatial neglect
Reference frames
Trunk rotation
Visuospatial temporal order judgment (TOJ)
Temporo-parietal junction (TPJ) laterality
Handedness
Ocular dominance
fMRI
Eye tracking

ABSTRACT

The rotation of the trunk around its vertical midline could be shown to bias visuospatial temporal judgments towards targets in the hemifield ipsilateral to the trunk orientation and to improve visuospatial performance in patients with visual neglect. However, the underlying brain mechanisms are not well understood. Therefore, the goal of the present study was to investigate the neural effects associated with egocentric midplane shifts under consideration of individual handedness. We employed a visuospatial temporal order judgment (TOJ) task in healthy right- and left-handed subjects while their trunk rotation was varied. Participants responded by a saccade towards the stimulus perceived first out of two stimuli presented with different stimulus onset asynchronies (SOA). Apart from gaze behavior, BOLD-fMRI responses were measured using functional magnetic resonance imaging (fMRI). Based on findings from spatial neglect research, analyses of fMRI-BOLD responses were focused on a bilateral fronto-temporo-parietal network comprising Brodmann areas 22, 39, 40, and 44, as well as the basal ganglia core nuclei (caudate, putamen, pallidum).

We observed an acceleration of saccadic speed towards stimuli ipsilateral to the trunk orientation modulated by individual handedness. Left-handed participants showed the strongest behavioral and neural effects, suggesting greater susceptibility to manipulations of trunk orientation. With respect to the dominant hand, a rotation around the vertical trunk midline modulated the activation of an ipsilateral network comprising fronto-temporo-parietal regions and the putamen with the strongest effects for saccades towards the hemifield opposite to the dominant hand. Within the investigated network, the temporo-parietal junction (TPJ) appears to serve as a region integrating sensory, motor, and trunk position information.

Our results are discussed in the context of gain modulatory and laterality effects.

1. Introduction

Goal-directed motor actions require the integration of visual, vestibular, and proprioceptive information into a body-centered, egocentric frame of reference (Cohen and Andersen, 2002; Colby, 1998). Brain regions involved in these multisensory integration processes are thought to be related to spatial attention and visuomotor planning, such as parietal and superior temporal cortices (Andersen et al., 1993; Brotchie et al., 1995; Crawford et al., 2011). The occurrence of spatial neglect following lesions in these, mostly right-hemispheric brain regions (Chechlacz et al., 2010; Chechlacz et al., 2013; Karnath et al., 2001) is compatible with this concept.

Spatial neglect is characterized by impairments in the ability to orient, perceive, and respond to stimuli in the contralesional hemifield (Chokron et al., 2007). Specifically, a strong bias of exploratory and voluntary movements towards the ipsilesional space is one of the core

* Corresponding author at: German Center for Addiction Research in Childhood and Adolescence, University Medical Center Hamburg-Eppendorf, Martinistr. 52, Hamburg 20246, Germany.
E-mail address: k.paschke@uke.de (K. Paschke).
[1] Torsten Wüstenberg and Melanie Wilke contributed equally.

https://doi.org/10.1016/j.nicl.2019.101898
Received 5 October 2018; Received in revised form 13 May 2019; Accepted 13 June 2019
Available online 22 June 2019

deficits of spatial neglect. It has been proposed that these dysfunctions result from a lesion-induced deviation of the egocentric trunk midline towards the ipsilesional hemifield (Fruhmann-Berger and Karnath, 2005; Karnath, 1997, 2015; Ventre et al., 1984). This midline-shift theory is supported by the reports of neglect patients who often perceive a shift of their trunk midline towards the ipsilesional side (Ferber and Karnath, 1999; Karnath, 1994). This experience seems to be associated with the occurrence of an ipsilesional spatial bias, as the pattern of exploratory eye movements is shifted towards the ipsilesional hemifield with respect to the *objective* trunk midline, while being symmetrical with respect to the *subjective* trunk midline (Hornak, 1992; Karnath et al., 1991). Furthermore, manipulations of the physical or perceived trunk midline (by neck muscle or caloric-vestibular stimulation) have been shown to reduce visual neglect symptoms (Chokron et al., 2007; Johannsen et al., 2003; Karnath et al., 1993; Karnath et al., 1996; Karnath et al., 1991; Li et al., 2014; Moon et al., 2006; Rode and Perenin, 1994; Måns Magnusson and Ba, 1999; Schindler, 2002; Schindler and Kerkhoff, 1997; Wilkinson et al., 2014). Physical or illusionary trunk rotation towards the contralesional side shortened saccade latencies towards the disturbed hemifield (Karnath et al., 1991), re-centered exploratory eye movement patterns, and improved the performance in visual detection even in the absence of an overt motor response (Karnath et al., 1993). In healthy subjects Fink et al. (2003) investigated the influence of the perceived body position via manipulation of the egocentric representation by galvanic vestibular stimulation. In their fMRI study, an interaction effect was found in the right posterior parietal and the right ventral premotor cortex while subjects solved an allocentric line-bisection task. Moreover, Brotchie et al. (2003) manipulated subjects' trunk orientation within the MR scanner. The authors demonstrated that a region in the human intraparietal sulcus responds to visual, saccadic, and memory components of saccade tasks with highest signal changes in the hemisphere ipsilateral to the side of trunk orientation. The main limitation of this interesting study is the low number of subjects and rotation conditions: only four out of six subjects had been rotated to the left and the right. Moreover, the fMRI-data acquisition and analysis were focused on the intraparietal sulcus excluding more ventro-parietal, superior temporal, as well as frontal regions likely involved in a trunk rotation sensitive network.

In order to study biases of spatial attention and oculomotor responses, the temporal order judgment task (TOJ) has proven to be a useful tool in neurological patients and healthy subjects (see e.g. Woo et al., 2009; Wada et al., 2004). In the current study, we used the visuospatial version of TOJ tasks: Two stimuli appear in the left and right hemifield of a screen with different stimulus onset asynchronies (SOA). Subjects are asked to indicate the first appearing stimulus by means of a directed saccade. Due to its hemifield specific and spatial attention related components, TOJ tasks are well suited for the investigation of neglect-associated deficits. Patients with lesions in the inferior parietal lobule (IPL) tended to perform ipsilesional saccades unless the contralesional target appeared substantially earlier than the ipsilesional stimulus (Ro et al., 2001; Rorden et al., 1997). In the latter study, patients required a lead on the order of 200 ms to judge the contralesional stimulus as having appeared simultaneously with the ipsilesional stimulus. A comparable prior-entry bias for visual targets presented in the right hemifield occurred after structural (following apoplectic insult) and transient functional right-hemispheric lesions induced by transcranial magnetic stimulation (TMS) (Arend et al., 2008; Baylis et al., 2002; Ro et al., 2001; Sinnett et al., 2007; Woo et al., 2009). In the mentioned studies, a right-hemifield spatial bias seems to be strongly connected to disturbances in the right hemisphere. Specifically, TMS application over the right posterior parietal cortex (PPC) of healthy individuals led to a delayed detection of visual targets in the left (contralateral) hemifield (Woo et al., 2009), while no effects were found when TMS was administered over the left PPC suggesting an influence of brain laterality. Complementing, stronger rightward prior-entry biases were found in healthy right- compared to healthy left-handed subjects (Efron, 1963; Geffen et al., 2000).

In a previous behavioral study we showed a trunk rotation and response-contingent impact of functional laterality (as indicated by handedness) in a visuospatial TOJ task in form of an ipsilateral prior-entry bias (Paschke et al., 2015). This trunk-rotation induced spatial bias was most pronounced in left-handed participants suggesting modulatory effects of functional laterality specifically during rightward trunk rotations. In addition, we observed an effect of ocular dominance on the TOJ bias: subjects with a right ocular dominance showed a rightward bias in the straight trunk orientation, while subjects with a left ocular dominance showed no initial bias. Taken together, functional laterality assessed by handedness and ocular dominance measures seems to affect visuospatial temporal order judgments and should be considered in the analysis of the underlying neuronal function.

The brain network we are interested in is most likely located within cerebral regions frequently associated with visuospatial neglect: the superior temporal gyrus (STG, BA 22), the angular gyrus (AG) of the inferior parietal lobule (IPL, BA 39), the ventral postcentral gyrus,the supramarginal gyrus (SMG, BA 40) at the temporoparietal junction (TPJ), and the pars opercularis of the inferior frontal gyrus as well as posterior parts of the middle frontal gyrus (BA44; Halligan et al., 2003; Harvey and Rossit, 2012; Jacobs et al., 2012; Karnath et al., 2001; Mort et al., 2003, Karnath et al., 2004; Karnath et al., 2011, Molenberghs et al., 2012). Karnath and Rorden (2012) emphasized the role of a perisylvian neural network with the inferior parietal lobule and the superior temporal cortex including TPJ (junction of BA22, BA 39, and BA 40) linking to one another as well as prefrontal regions. Although neglect after left hemispheric injury is less frequent and not as severe, corresponding lesions were found to be associated with similar contralesional symptoms (Kleinman et al., 2007; Suchan et al., 2012).

Additional to the already mentioned cortical sites, two lesion-symptom-mapping studies by Chechlacz and colleagues (Chechlacz et al., 2012b; Chechlacz et al., 2012a), highlight the role of basal ganglia damages in neglect. Specifically, lesions in the putamen and caudate ipsilateral to the dominant hand were found to be associated with egocentric symptoms. Considering these findings, we also included the core nuclei of the basal ganglia in our network of interest.

An investigation and experimental manipulation of activity within the described network in the healthy, i.e. not damaged brain may help to get a better understanding of the neural processes underlying neglect symptoms. Interestingly, neurons in posterior parietal and prefrontal cortices were discovered whose firing rates are modulated by the position of eyes, head, and body (gain modulation, Andersen and Gnadt, 1989; Cohen and Andersen, 2002; Lehky and Tanaka, 2016). This finding suggests that oculomotoric, proprioceptive, and vestibular information contributes to individual spatial referencing (Brotchie et al., 2003).

Therefore, the aim of the present study was to investigate neuronal activation changes induced by physical trunk rotation during temporal order judgments. To this end, we employed a visual temporal order judgment task with differing trunk rotations in a combined event-related fMRI-eye tracking design and accounted for the influence of individual hand preference. We focused on the regions known from lesion studies of visual neglect including fronto-parieto-temporal brain areas (BA 22, BA 39, BA 40, BA 44) as well as the basal ganglia core nuclei (caudate, putamen, pallidum).

We hypothesized that an influence of trunk rotation leads to neural activation changes in these regions with higher activation in the hemisphere ipsilateral to the trunk orientation (Brotchie et al., 2003). Moreover, we hypothesized the neural activation changes to be modulated by the direction of the saccadic response. For right-handed subjects we expected a more right-hemispheric lateralization whereas for left-handed subjects we expected a more heterogeneous pattern (Dieterich et al., 2003; Fink et al., 2003; Petit et al., 2015; Wada et al., 2004; Whitehouse and Bishop, 2009).

Table 1
Sample characteristics.

Handedness	N	Female N	Median age (years)	Age range (years)	Ocular dominance (right/left)	Median Edinburgh LQ (range)
Right-handed	12	8	25.5	21–30	9 R / 3 L	100 (67–100)
Left-handed	12	7	23	19–36	6 R / 6 L	−75 (−17 to −100)

2. Methods

2.1. Participants

Twenty-five volunteers without neurological illness and normal or corrected to normal visual acuity participated in our study. One subject (right-handed, RH) had to be excluded from further analysis due to technical difficulties during data acquisition. Thus, we report data from 12 right-handed (RH) and 12 left-handed (LH) subjects (see Table 1). Both handedness groups did not differ significantly with respect to gender (Chi-square test: χ^2 (1) = 0.18, p = 1) or age (two-tailed t-test for independent samples: T(23) = 0.15, p = 0.882). Subjects were paid for their participation and could earn an additional bonus according to their performance on trials with maximum SOA (to increase overall motivation).

All subjects gave written informed consent to participate in the experiments. The study was approved by the local Ethics Committee of the Georg-August-University Göttingen and conducted according to the Declaration of Helsinki.

2.2. Assessment of handedness and ocular dominance

Dominant hand: Individual handedness was assessed with the Edinburgh Inventory (Oldfield, 1971). Based on the evaluation of everyday hand use, the Edinburgh laterality quotient (LQ) was computed, ranging between −100 (maximum left-hand dominance) and 100 (maximum right-hand dominance). Subjects were rated as left-handed with a LQ < 0 and right-handed with a LQ > 0 (Oldfield, 1971). Right-handed subjects had a median LQ score of 100 (LQ range [67100], median decile R.10, decile range [R.3 R.10]). Left-handed participants had a median LQ score of −75 (LQ range [−17–100]), median decile L.6, decile range [L.1 L.10]).

Dominant eye: Ocular dominance was determined using a variant of the Porta test (Li et al., 2010). Subjects were asked to hold a pen vertically with both hands and extended arms and to align the pen with a distant corner of the room (4 m away). Participants were then asked to close one eye after the other and report which eye closure led to the largest pen-corner misalignment. This eye was assumed to be the dominant eye.

25% of the right-handed and 50% of the left-handed subjects showed left-eye dominance (Table 1). This proportion is in agreement with previous studies (Annett, 2000; McManus, 1999; Petit et al., 2015).

2.3. Experimental set-up

2.3.1. Behavioral task

Participants performed a similar visual temporal order judgment (TOJ) task as in the behavioral study we described in a former paper (Paschke et al., 2015) adopted for the fMRI setup.

Within an experimental trial, two small white filled squares with a side length of 0.5° visual angle were presented at eccentricities of ± 15° visual angle on the horizontal meridian (left or right hemifield) either simultaneously or with a stimulus onset asynchrony (SOA) of 17 or 300 ms (Fig. 1B). Subjects were requested to perform a saccade towards the stimulus that had appeared first (target) as fast and as correctly as possible (even in case of simultaneous presentation). Trials with simultaneous presentation and trials with a SOA of 300 ms were repeated 56 times each. Trials with a SOA of 17 ms were repeated 28 times. In total this led to 140 trials per run. In case of an onset asynchrony, targets appeared first at the left or right hemifield with equal probability. All trial types were presented in random order.

The aforementioned differences in trial number are intended to ensure the best possible balance between the duration of the experiment and the goodness of psychometric and BOLD-response modeling. Because the main focus of our experiment was the investigation of brain responses, the frequency of trials important for an adequate subject level BOLD-modeling (trials for the quantification of the initial bias: simultaneous presentation, and trials with probably always correct judgments: SOA of 300 ms) were threefold higher than those of trials with a high degree of uncertainty in judgment (SOA of 17 ms), only important for the psychometrical modeling.

Participants lay in the scanner within a darkened surrounding. Depending on the experimental condition, they were lying on their back (trunk oriented straight), on the side rotated 45° to the left or 45° to the right around the trunk's vertical axis. In all trunk rotation conditions, head and eyes were facing straight ahead (Fig. 1C). The body was supported by stabilizing wedge-shaped pillows to hold position fixed by straps. The head was stabilized by pillows filling out the head coil. Between runs, subjects were unlocked and took a small break to stretch and relax their muscles. Then they were re-positioned on the table and within the head coil. One run within a given trunk position lasted about 15 min. Including task introduction outside and inside the scanner, the assessment of handedness and ocular dominance, as well as the short break, the re-positioning of the subject in-between runs and the re-calibration of the eye-tracker, the experiment lasted about 1 h and 30 min for each subject. The order of the trunk orientations was pseudo-randomized between subjects to exclude orientation-associated order effects.

Each trial started with the presentation of a central fixation cross. As in our previous experiment (Paschke et al., 2015) the presentation of all trials was eye-movement controlled: Stimuli appeared only when the subject fixated the central cross properly for 400 ms within a radius of 5°. With the appearance of the (first) stimulus the fixation cross was turned off simultaneously. Trials that were not answered by a proper saccade followed by a fixation of the target for at least 200 ms within a 5° radius and within 1 s, were aborted. At the end of each run, a feedback and a bonus were given based on the proportion of valid and correctly performed trials with a SOA of 300 ms (even though subjects believed that it was feedback for all SOAs). Feedback and bonus were included to enhance subject's motivation to keep a good performance for the whole duration of the experiment. Due to the temporal properties of the BOLD response, the inter-trial-intervals (ITIs) were set to 6 to 10 s to allow a nearly complete return of the BOLD response to the baseline (Fig. 1A).

2.3.2. Brain imaging

2.3.2.1. Data acquisition. MR scans were acquired on a 3.0 Tesla Siemens Magnetom Trio equipped with a twelve-channel phased array head coil. First, 3D T1-weighted structural images were acquired (Magnetization Prepared Rapid Acquisition Gradient Echo pulse sequence - MPRAGE, voxel size = 1 × 1 × 1 mm^3, echo time (TE) = 4 ms, repetition time (TR) = 1950 ms, flip angle (FA) = 14°). Afterwards, 448 ± 17 T2*-weighted, blood-oxygenation level sensitive (BOLD), whole head functional brain images were collected using a 2D-gradient echo echo-planar pulse sequence (GE-EPI, voxel size of

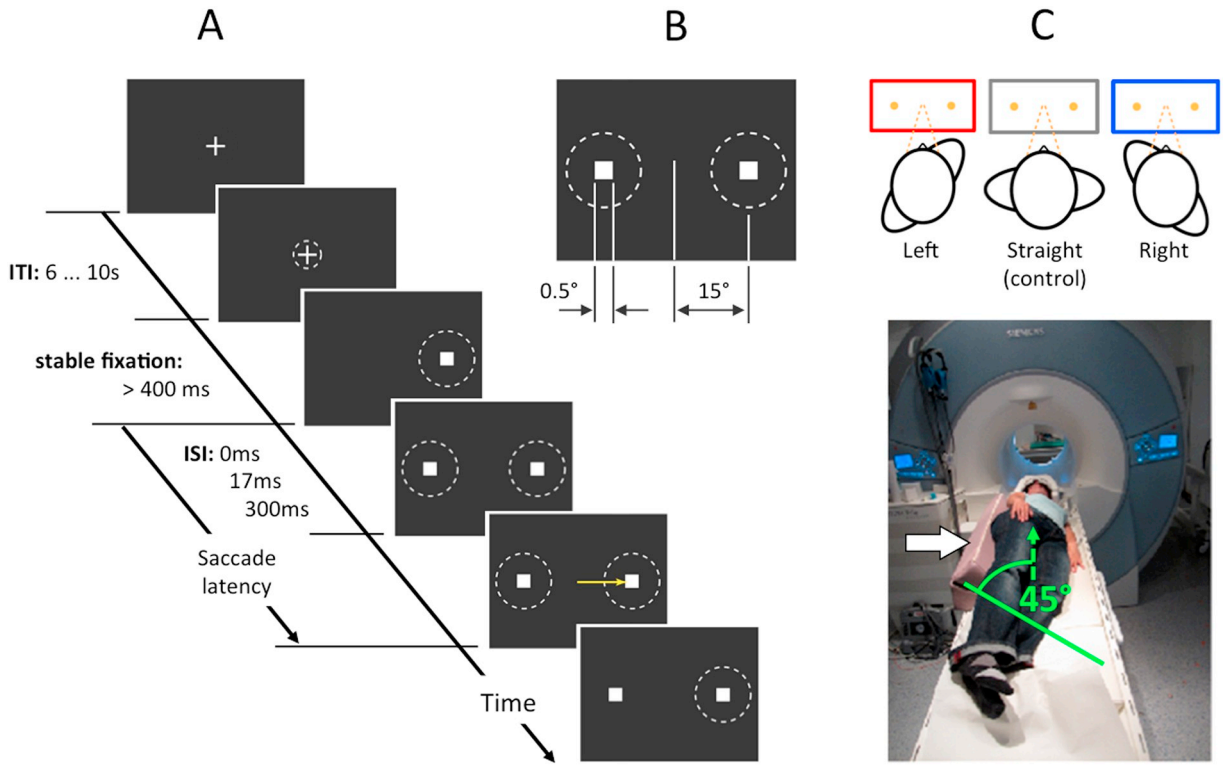

Fig. 1. Experimental set up. (A) Experimental task and timing: The yellow arrow denotes the saccade towards the target. (B) Stimulus configuration (all values are given in degrees of visual angle). (C) Scanner set up: The photograph shows an exemplary leftward trunk rotation inside the magnet stabilized by two wedge-shaped pillows placed in the back of the participant (white arrow). This results in a trunk rotation of about 45° (green line). Participants' head position remained always straight (dashed green arrow). Above the photo, the color-coding of trunk rotation levels is shown in a schematic display. (For interpretation of the references to color in this figure legend, the reader is referred to the web version of this article.)

$3 \times 3 \times 4\,mm^3$, TE = 30 ms, TR = 2000 ms, FA = 70°, 33 interleaved slices in ascending acquisition order). To guarantee an optimal slice positioning before data acquisition and an optimal coregistration of MR-images between the runs during image preprocessing, we acquired a separate structural image for each of the three experimental runs.

2.3.2.2. Stimulus presentation. Stimuli were generated using Presentation® software (Neurobehavioral System Inc., version 16.2, www.neurobs.com) and presented on a MRI-compatible VisuaStim® digital goggle system (Resonance Technology, Inc.; http://www.mrivideo.com/). The goggles contained two thin-film-transistor (TFT) displays with an optical resolution of 800 × 600 pixels covering a visual field of 32° horizontally and 24° vertically. The displays had a vertical refresh rate of 60 Hz. Real-time eye tracking was performed with a fMRI compatible ViewPoint® eye tracker (Arrington Research) running on a separate PC. Gaze position was sampled continuously with a temporal resolution of 60 Hz with an IR sensitive camera placed below the subjects' right eye, transferred to the Presentation PC using the ViewPointClient Ethernet Interface and recorded together with stimulus and timing information. At the beginning of each experimental run the eye tracker was calibrated using a 4 × 5 matrix.

2.4. Analysis

2.4.1. Analysis of behavioral data

The analysis of the behavioral data was performed analogous to our previous experiments (Paschke et al., 2015). Due to the task adaption to the fMRI design with smaller stimulus eccentricities, lower degree of body rotation, longer inter-trial-intervals (ITIs), less trial repetitions, and the supine position of the subjects, we assumed lower task sensitivity. Choice behavior was analyzed by means of psychometric modeling. We estimated the psychometric function for each participant and trunk rotation separately (see Supplementary Fig. 1A). To this end, a logistic function.

$$f(x) = \gamma + (1 - \gamma - \lambda)\, p(x), \text{ where } p(x) = 1/(1 + 10^{-\beta*(x-\alpha)}), \quad (1)$$

was fitted to the choice data (probability of selecting the right target as a function of SOA, R, https://stat.ethz.ch, psyphy package, https://stat.ethz.ch/R-manual/R-patched/library, version 0.1–9, (Klein, 2001; Wichmann and Hill, 2001), function parameters: γ - lower asymptote value, λ - upper asymptote value, α - point of inflection, β – slope at α). Model accuracy was assessed by means of goodness-of-fit coefficients (pseudo R^2) for individual subjects of both handedness groups. According to the significant results from our previous study, we focused on one key parameter estimated from the psychometric functions of each subject in order to test whether a replication of the results was possible despite the different experimental setup conditions:

The point of subjective simultaneity (PSS) reflects the time interval by which one stimulus has to precede (or follow) the other in order for the two stimuli to be perceived as simultaneous. The objective point of simultaneity in the TOJ task is at SOA = 0 ms (i.e. left and right stimulus appear simultaneously). A non-zero PSS indicates that one of the two stimuli has to lead in time to be chosen equally often. The probability of right choice was plotted as a function of SOA. A leftward shift of the psychometric function with a resulting negative PSS indicates a bias towards "right first" reports. Conversely, a positive PSS indicates a bias towards "left first" responses, as the right target has to precede the left target to be judged as simultaneous (see Supplementary Fig. 1B).

Besides PSS, common quoted parameters of the psychometric function are thresholds and the just noticeable difference (JND) (Spence and Parise, 2010). We refer to those in the Supplementary Material (Supplementary Fig. 3, Supplementary Table 1).

2.4.2. Eye movement analysis

We analyzed saccade latency for each subject's responses after the target onset: The saccade latency was determined for each individual trial. Eye position traces were interpolated to a temporal resolution of one millisecond and differentiated to obtain the saccade velocity. We identified and eliminated outliers (e.g. blinks) by excluding

z-transformed velocity values $-3 < z > 3$. The beginning of a saccade was detected when the velocity reached 0.05°/ms after a minimum response latency of 4 screen frames (66.67 ms). Thus, the latency indicates the time interval between the target onset and the beginning of the saccade. Latency values were included in a 3 × 2 repeated-measures analysis of variance (rANOVA) with the within subject factors *trunk rotation* (left/straight/right) and *saccade direction* (left/right). When appropriate, a Greenhouse-Geisser correction of the degrees of freedom was applied. Significant main effects and interactions were further analyzed by pairwise *t*-tests applying Bonferroni-corrections if required.

Influence of handedness: We previously showed an influence of handedness on trunk rotation effects. Thus, in line with our earlier behavioral study, all analyses were performed for left- and right-handed subjects separately.

Influence of ocular dominance: Whereas ocular dominance modulates a prior entry bias of left and right hemifield stimuli in the non-rotation condition, it could not be shown to be a major contributor to the effect of trunk rotation (Paschke et al., 2015). According to our prior behavioral results it was assumed that subjects with right ocular dominance show smaller PSS values than subjects with left ocular dominance in the straight trunk orientation. PSS for left and right ocular dominant subjects in the straight trunk orientation was compared using a non-parametric one-sided two-sample Wilcoxon rank sum test.

2.4.3. Analysis of fMRI data

2.4.3.1. Image preprocessing and artifact reduction. Data analysis was conducted using Statistical Parametric Mapping (SPM12, Wellcome Department of Imaging Neuroscience, London, UK, http://www.fil.ion.ucl.ac.uk/spm/). First, structural images of the second and third experimental runs were coregistered to the first structural image and the transformation parameter estimates were applied to the corresponding functional images. Functional images were then corrected for acquisition delay and head motion. To eliminate residual differences in image orientation, a mean structural image was computed and coregistered to the mean functional image computed after artifact correction. The mean structural image was than segmented into tissue classes using the unified segmentation algorithm provided by SPM12 (Ashburner and Friston, 2005). Functional and structural images were warped into a stereotactic reference space (International Consortium for Brain Mapping, ICBM; http://www.loni.ucla.edu/ICBM/) using the warping parameters estimated during the segmentation process, resampled into isotropic voxels (voxel size = 3 × 3 × 3 mm^3) and spatially smoothed using an isotropic Gaussian kernel (full width half maximum, FWHM = 8 mm).

2.4.3.2. Quality assessment. Our unusual design with three "independent", condition-associated scanning sessions and with different positions of the participant within the magnet is more vulnerable to scanning artifacts than conventional, multi-run designs. Thus, in addition to the well-established preprocessing pipeline described in the former paragraph, we inspected our data regarding differences in head motion, paradigm correlated head motions, and differences in local signal-to-noise ratio within our ROIs. For a detailed description of the used analyses and the findings see supplementary material (supplementary methods III & IV and supplementary results V & VI).

2.4.3.3. Modeling of individual brain responses to the experimental task. Statistical analyses were performed within the framework of the Generalized Linear Model (GLM). At the first stage, individual neural activity was modeled by a stick function for each experimental trial. The corresponding BOLD model was obtained by convolving these stick functions with the canonical hemodynamic response function (HRF) as implemented in SPM. The resulting time courses were down-sampled for each scan to form explanatory variables. The final model consisted of 6 explanatory variables of interest per run (trunk rotation condition): 3 stimulation conditions x 2 saccade directions. In case of aborted trials (see Methods Section 2.3), these trials were modeled separately and included as regressors of no interest. Moreover, to account for signal fluctuations due to susceptibility x motion interactions, the six movement parameters estimated during the motion correction step were considered as additional regressors of no interest.

Before fitting the model to the data, low frequency signal drifts in voxel time series were eliminated by means of a high pass filter with a cutoff frequency of 1/128 Hz. Physiological noise due to respiratory or aliased cardiologic effects was removed by means of autoregressive modeling. Weighting parameters of the GLM were then estimated by restricted maximum likelihood (ReML) fit. Moreover, linear contrast images were computed for the conditions of interest for each subject and submitted to separate group level analyses for left- and right-handers.

2.4.3.4. Network of interest (NOI). Due to our strong a-priori anatomical hypotheses regarding spatial neglect-relevant brain regions and according to the ALE meta-analysis of Molenberghs et al. (2012), we restricted the models to voxels within a network of interest (NOI) composed of Brodmann areas (BA) 22, 39, 40 and 44 as well as of the basal ganglia core nuclei caudate, putamen, and pallidum bilateral (see Fig. 2 for more details). BA22 covers large parts of superior temporal gyrus (STG) except its most anterior proportion. BA39 covers the inferior parietal lobule (IPL) including parts of the angular gyrus (AG) and the temporo-parietal junction (TPJ). BA 40 covers more superior portions of the parietal lobe including the supramarginal gyrus and parts of TPJ as well. BA44 includes pre-motor structures, specifically posterior proportions of the middle frontal gyrus (MFG) and the opercular portion of the inferior frontal gyrus (IFG).

The NOI-mask used in our group level analyses was computed by a voxel-wise logical OR operation applied to these brain structures derived from the digital Brodmann brain atlas as implemented in MRIcroN (www.mccauslandcenter.sc.edu/crnl/mricron/) and from the high-resolution probabilistic in vivo atlas of human subcortical brain nuclei published by Pauli et al. (2018). Although the majority of neglect-associated lesions are located in the right cerebral hemisphere, we included also the homologous regions of the left hemisphere to address possible brain laterality differences in our left-handed subsample.

2.4.3.5. Group level statistics. At the second stage, repeated measures analyses of covariance (rANCOVAs) were conducted for left- and right-handed participants separately. Additionally, all subjects were included in one model to illustrate activations associated with the visuospatial TOJ task. The analyses contained the within subject factors *trunk rotation* (left rotation, straight orientation, right rotation) and *saccade direction* (right or leftward saccade) as well as the covariate ocular dominance. Alpha error probabilities were corrected based on the random field characteristics of the resulting statistical parametrical map within the NOI. The statistical threshold was set to $p < 0.05$ family wise error (FWE) corrected for multiple comparisons and a minimum cluster size of 10 adjacent voxels (270 mm^3).

Additionally, a whole-brain analysis was carried out without a-priori masking for left- and right-handed subjects separately. Results are provided in the supplementary material (supplementary results VII).

2.4.3.6. Laterality analyses. Laterality analyses were restricted to the cortical nodes of our NOI. For the assessment of differences in

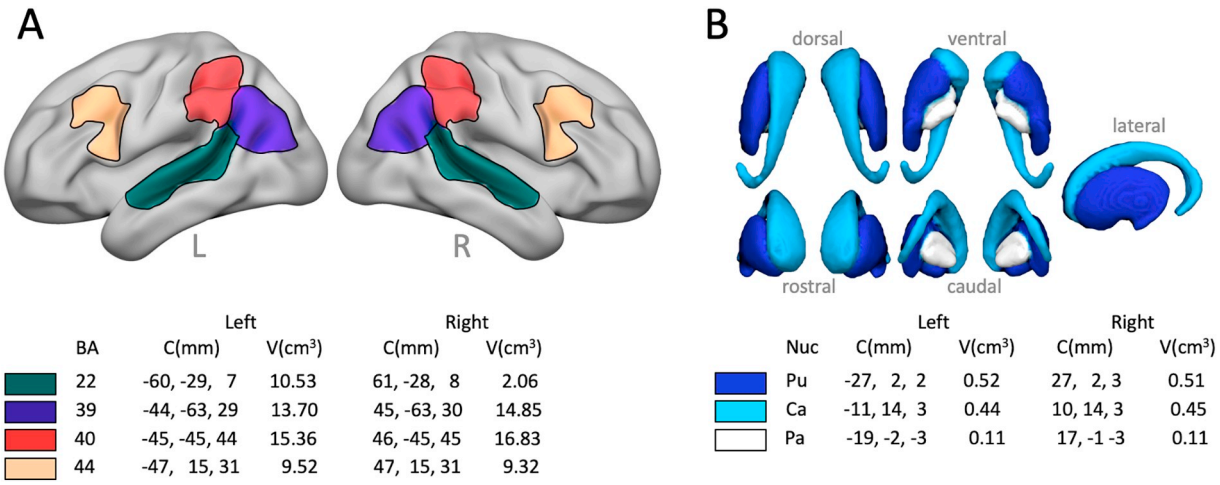

		Left		Right	
	BA	C(mm)	V(cm³)	C(mm)	V(cm³)
	22	-60, -29, 7	10.53	61, -28, 8	2.06
	39	-44, -63, 29	13.70	45, -63, 30	14.85
	40	-45, -45, 44	15.36	46, -45, 45	16.83
	44	-47, 15, 31	9.52	47, 15, 31	9.32

		Left		Right	
	Nuc	C(mm)	V(cm³)	C(mm)	V(cm³)
	Pu	-27, 2, 2	0.52	27, 2, 3	0.51
	Ca	-11, 14, 3	0.44	10, 14, 3	0.45
	Pa	-19, -2, -3	0.11	17, -1 -3	0.11

Fig. 2. A-priori defined cortical network of interest (NOI). (A) Brodmann areas 22, 39, 40, and 44 bilateral as defined by the digital Brodmann brain atlas implemented in MRIcroN (www.mccauslandcenter.sc.edu/crnl/mricron/). Cortical network nodes are shown overlaid on a slightly inflated and smoothed cortical surface of the cerebrum as provided by the Open GL software package Surf Ice (https://www.nitrc.org/projects/surfice/). (B) Basal ganglia ROIs as defined in the high-resolution probabilistic in vivo atlas of human subcortical brain nuclei published by Pauli et al. (2018). The nuclei specific color coded, joint basal ganglia ROI is shown in different views. Below the ROI images, center coordinates and volumes of the single structures are listed for the left and right cerebral hemisphere separately. The caudate values concern the head of the nucleus. Abbreviations: BA – Brodmann area, Nuc – Nucleus, Pu – Putamen, Ca – Caudate, Pa – Pallidum, C – center coordinate in MNI space, V – volume, L – left, R – right. (For interpretation of the references to color in this figure legend, the reader is referred to the web version of this article.)

hemispheric sensitivity to the TOJ task, we computed laterality indices (LIs) for the BAs forming our NOI. LIs were computed according the recommendations of Seghier (2008).

$$LI^{BAj} = \frac{BR_L^{BAj} - BR_R^{BAj}}{|BR_L^{BAj}| + |BR_R^{BAj}|} \quad (2)$$

with brain response $BR_{L/R}{}^{BAj}$ in Brodmann area $j \in [22, 39, 40, 44]$ of the left or right hemisphere as estimated by the parameter weights of the individual models and adjusted for the effect of the dominant eye. Because we conducted this analysis for our six experimental conditions separately, we obtained $6 \times 4 = 24$ LI-values for each subject. The statistical significance of the hemispheric lateralization indices was than assessed using non-parametrical Wilcoxon signed rank tests.

2.4.3.7. Data presentation. For display purposes, we mapped the results of our analyses onto a slightly inflated and smoothed cortical surface of a cerebrum in stereotactical standard space as provided by the Open GL software package Surf Ice (https://www.nitrc.org/projects/surfice/). For the display of subcortical effects, we reconstructed the outer surface of the basal ganglia nuclei group consisting of putamen, caudate and pallidum. Subcortical effects were than overlaid on this surface also using the Surf Ice software. Additionally, the mean parameter estimates at peak position are shown. Finally, we created color-coded LI matrices. All results are presented for left- and right-handers separately.

3. Results

Our fMRI experiment aimed to investigate how physical trunk rotation affects neuronal activation patterns in neglect-associated fronto-parieto-temporal brain regions during visuospatial temporal order judgments (TOJ) and how individual differences in functional laterality as measured by handedness modulate these effects. Analogous to our previous behavioral experiment (Paschke et al., 2015), we present data separately for right- and left-handed groups, and directly compare them at a later part of the results section. The reason for the initial separation of the two handedness groups is to ensure comparability with previous studies on trunk rotation effects, since most studies in neglect patients as well as in healthy controls included predominantly right-handed subjects.

3.1. Behavioral results

3.1.1. Effect of ocular dominance

Apart from handedness – which reflects motor laterality in humans – ocular dominance is another, more perception related measure of functional laterality. In line with previous studies (Bourassa et al., 1996), the left-handed group contained an equal amount of left-eye dominant ($n = 6$) and right-eye dominant (n = 6) subjects, while right-handed subjects exhibited mostly right-eye dominance (9 of 12 subjects).

Analogous to our behavioral paper we first characterized TOJ performance in the straight trunk condition. To this end, we calculated the proportion of 'right-first' choices as a function of SOA and determined the *point of subjective simultaneity* (PSS) individually for right ($N = 15$) and left-eye dominant ($N = 9$) subjects (see Methods Section 2.5.1). Previously, we could show an influence of eye-dominance on the PSS with an initial pre-entry bias for right hemifield stimuli for right, as compared to left ocular dominant subjects (Paschke et al., 2015). Accordingly, right-eye dominant subjects showed a negative PSS (mean − 14.34 ms, S.D. 25.7 ms, one-sided one-sample Wilcoxon rank sum test: $U = 28$, $p = .036$) indicating a prior entry bias for right targets, while left-eye dominant subjects had a PSS ranging around zero (mean 0.34 ms, S.D. 34.8 ms, $U = 26.5$, $p = .34$, Fig. 3A). Although the PSS in the straight-ahead condition was significantly negative in the right-ocular dominant group, it just differed between the two groups in trend ($U = 43.5$, $p = .079$).

Taken together, these results are in line with the results from our previous behavioral study: ocular dominance is linked to a shift of the PSS towards the dominant eye.

3.1.2. Effect of trunk rotation

Besides PSS we analyzed the *saccade* latency in all experimental conditions. The mean values for all trunk rotations are provided in Supplementary Table 1.

Left-handed group: Fig. 3B illustrates the psychometric curves for left-handed subjects. Inspection of the psychometric functions indicates a shallower slope in rightward trunk rotation due to lower sensitivities for left and right choices. The rANOVA revealed no effect of *trunk rotation* on PSS ($F(2,22) = 0.32$, $p = .73$, Supplementary Fig. 3).

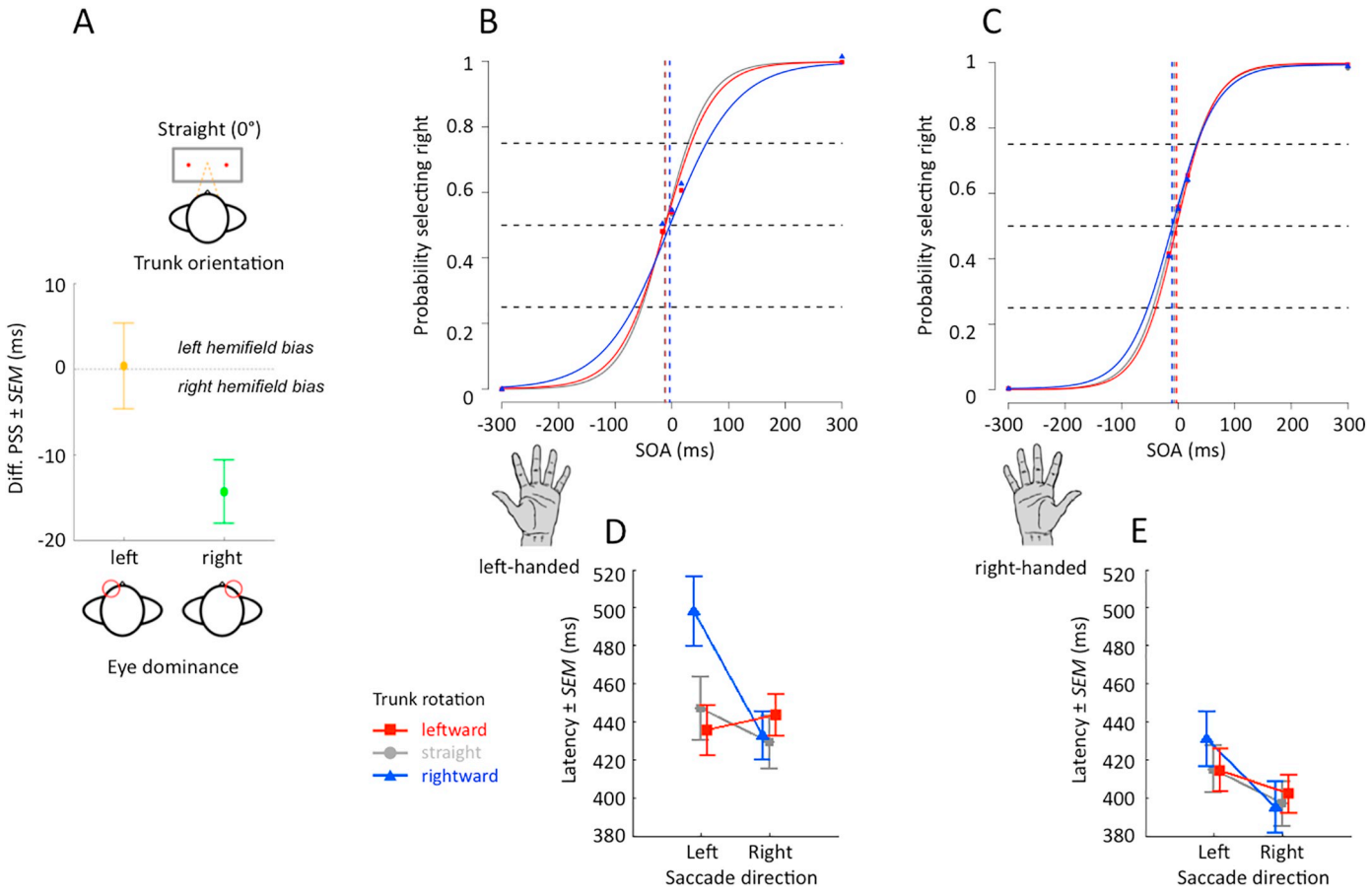

Fig. 3. Behavioral findings. (A) Eye dominance related bias point of subjective simultaneity (PSS). Displayed are mean differences in PSS and its standard errors. Note the right hemifield bias in right-eyed subjects. (B & C) Subjects' behavior was modeled by fitting a logistic psychometric function to the data (stimulus onset asynchrony vs. probability selecting right target). A negative SOA denotes a leading left stimulus. Threshold values for the different trunk rotations are displayed as vertical dashed lines in the same color as the associated psychometric functions. (D & E) Mean saccade latencies. (For interpretation of the references to color in this figure legend, the reader is referred to the web version of this article.)

However, for the saccade latency we found a significant interaction effect of *trunk rotation x stimulus choice* ($F(2,22) = 3.54$, $p < .05$). A post-hoc pairwise comparison of left and right stimulus choices in each trunk orientation revealed that the rightward trunk rotation led to a slowing down of leftward saccades compared to rightward saccades (mean latency right choice: 432.54 ms, S.D. 63.13; mean latency left choice: 467.9 ms, S.D. 44.29; $T(11) = -2,67$, $p < .05$; Fig. 3D).

*Right-handed group:*Fig. 3C illustrates the mean psychometric curves for right-handed subjects, separated by *trunk rotation*. Inspection of the psychometric fits suggested that rightward rotation was associated with a reduced probability of left targets being reported as leading (cf. Fig. 4B, blue curve). However, no statistically significant effects could be found for PSS ($F(2,22) = 0.45$, $p = .64$). When looking at the latency in a two-factorial rANOVA to investigate possible effects of *trunk rotation* as well as *stimulus choice* (left or right), and a possible interaction effect, an influence of the saccade direction could be detected ($F(1,11) = 9.03$, $p > .05$). Right-handed subjects showed faster saccades when choosing right hemifield stimuli compared to left hemifield stimuli irrespective of trunk orientation (mean right choice: 397.86 ms, S.D. 43.38; mean left choice: 419.96 ms, S.D. 40.43; $t(11) = 3.01$, $p = .01$). Neither an effect of *trunk rotation* on the latency ($F(2,22) = 0.09$, $p = .91$) nor an interaction effect of *trunk rotation* and *stimulus choice* could be revealed ($F(2,22) = 1.71$, $p = .21$; Fig. 3E).

To summarize the effects of trunk rotation in both handedness groups: 1) Rightward trunk rotation induced a significant deceleration of left choice saccades during temporal order judgments in left-handed subjects. Thus, saccade latency could be shown to be a sensitive measure for trunk rotation induced effects. 2) In right-handed subjects faster right choice saccades could be observed independently of trunk rotation. 3) In the present task design trunk rotation did not affect PSS in either handedness group suggesting lower task sensitivity due to the experimental design compared to our previous study (supine position, reduced target eccentricity, greater ITIs, less trial repetitions).

3.2. Brain imaging results

3.2.1. Effect of task set on brain responses

Irrespective of our experimental factors trunk rotation and saccade direction, the visuospatial TOJ task requires the subjects to perform saccades in every trial. Those include a rapid eye movement from a central fixation cross to the stimulus subjectively perceived first out of two peripheral stimuli presented either simultaneously or with a temporal delay. Thus, the effect of task set describes brain responses rather associated with this stable property of our experiment than the modulation of brain activity by our experimental conditions. In this sense, we investigated the brain response associated with *all* saccades by computing the corresponding F-contrast for left- and right-handed subjects separately.

In general, in both cerebral hemispheres the dorsal and ventral visual pathway as well as saccade control regions responded pronounced to all experimental conditions. In detail, in both handedness-groups the task lead to activation of regions associated with the performance of saccades and visual perception (Jamadar et al., 2013; Pierrot-Deseilligny et al., 2004). Those comprised frontal regions including the

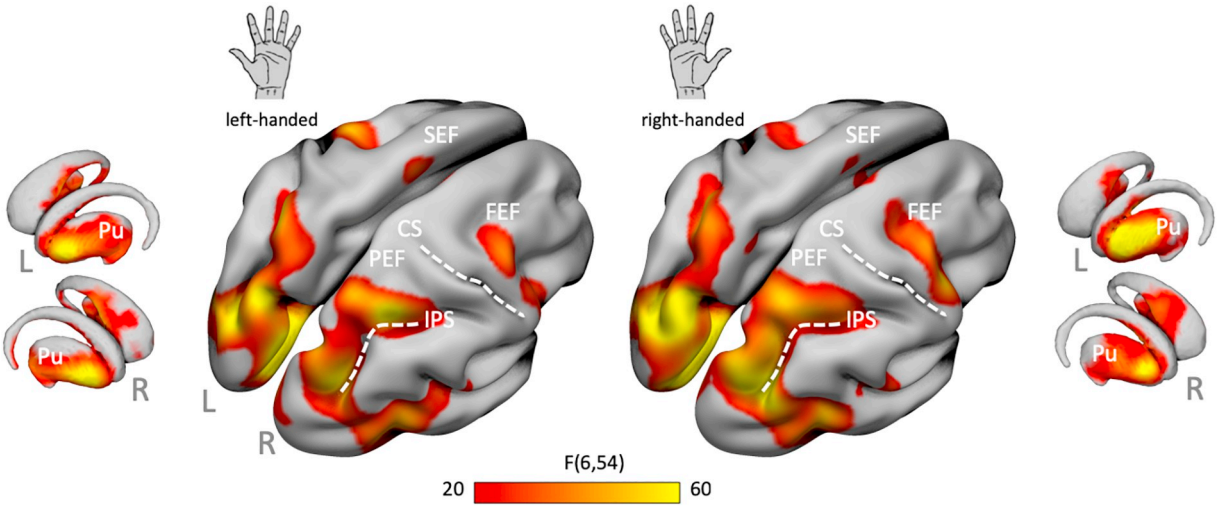

Fig. 4. Effect of task on fMRI BOLD responses. Condition independent cortical activation is displayed for left- and right-handed participants separately. Results of voxel-wise whole brain F-tests on the effects of interest (EoI, all experimental conditions). Abbreviations: L – left, R – right, SEF – supplementary eye field, FEF – frontal eye field, PEF – parietal eye field, CS – central sulcus, IPS – intraparietal sulcus, Pu – putamen.

supplementary eye field (medial frontal gyrus), a region close to the frontal eye fields (inferior and frontal gyrus), parietal regions including an area close to the parietal eye fields (precuneus, superior parietal lobule), as well as occipital regions including the calcarine, the middle and superior occipital gyrus. Moreover, temporal regions (left middle temporal gyrus), the middle cingulate cortex, the left thalamus including the pulvinar as well as large proportions of the putamen and – to a smaller extend – also the caudate head were activated by the task (Fig. 4).

3.2.2. Quality assessment

The in-depth analyses of head motion parameters estimated during the motion correction revealed a dependence of head motions on trunk rotation with significantly less z-translations as well as less pitch and roll rotations in the rightward rotation condition (see Supplementary Tables 3, 4a & b and Supplementary Fig. 5). However, no paradigm correlated head motions could be found; neither for the absolute head displacement as implemented as covariate in the single subject design matrices nor for the between scan head motion (all mean $r_{Pearson} < 0.1$, see Supplementary Figs. 6 & 7).

The analyses of trunk orientation dependent differences in local SNR revealed significant effects ($p_{FWE} < 0.05$) in the middle proportion of left BA22 for both handedness sub groups and in addition for right handers in the anterior part of right BA22, the inferior part of right BA44 and the right putamen/caudate (see Supplementary Table 5 and Supplementary Fig. 9).

3.2.3. Main effect of trunk rotation on brain responses

Trunk rotation modulates brain responses in ***BA44*** (LH & RH). Beside this, we observed additional effects in ***BA39*** (LH only) and ***BA22*** (RH only). Interestingly, the effects were exclusively located in the hemisphere opposite to the dominant hand. In detail:

Trunk rotation affects brain responses in *LH* subjects ***in left ventral BA44*** ($F_{(2,54)} = 21.57$, $p_{(FWE)} < 0.001$) with highest activations within rotation to the right (L < S < R). In the left-handed group we also found a main effect of trunk rotation in ***left ventro-rostral BA39 near TPJ*** ($F_{(2,54)} = 17.34$, $p_{(FWE)} = 0.004$).

In the *RH-group*, the ***right dorsal BA44*** showed a trunk rotation dependent effect in BOLD response ($F_{(1,54)} = 14.63$, $p_{(FWE)} = 0.018$). This effect was mainly driven by the differences between the straight and rotated trunk orientation with elevated brain responses for the latter. Interestingly, the direction of trunk rotation did not matter. In other words, compared to straight orientation we found elevated brain responses in this area for the rotation of trunk to the left as well as to the right. In contrast, in the ***right middle part of BA22*** we found a main effect ($F_{(2,54)} = 17.10$, $p_{(FWE)} = 0.005$), caused by a significantly elevated brain response during leftward trunk rotation.

In the LH group, the left putamen/caudate head showed trunk rotation dependent activity ($F_{(2,54)} = 12.91$, $p_{(FEW)} = 0.026$). Compared to the straight position, the brain response in these nuclei were elevated during rightward trunk rotation.

For more details about the direction of effects (as assessed by post-hoc *t*-tests for dependent samples) and a graphical display see Table 2 (upper part) and Fig. 5.

3.2.4. Interaction effects in brain responses

The test on interactions between saccade direction and trunk rotation revealed a complex pattern. Specifically in bilateral ***BA39*** we observed several modulatory effects for both handedness-groups, most pronounced in the left hemisphere and for rightward trunk rotation. In addition, neural activity in ***BA40*** (LH & RH) and ***BA22*** (RH only) was influenced by trunk rotation as well as saccade direction. Neither left- nor right-handed subjects showed any interaction effect in BA44.

The *LH-group*, showed a spatially extended and pronounced *interaction* in the left ***caudal part of BA39*** ($F_{(2,54)} = 26.12$, $p_{(FWE)} < 0.001$) and - to a lesser degree - also in the right hemisphere ($F_{(2,54)} = 11.56$, $p_{(FWE)} = 0.023$). The greatest difference in brain activity was found in left BA39 for rightward trunk rotation with elevated responses for saccades to the right. Interestingly, also in the straight condition saccades to the right were associated with stronger responses in both hemispheres. Beside these findings, a further interaction effect was found in the ***dorso-caudal part of left BA40*** ($F_{(2,54)} = 14.18$, $p_{(FWE)} = 0.005$). This effect was mainly driven by the inverse pattern of saccade direction x trunk rotation relation for the rotated conditions and the straight orientation. However, effects in right BA39 and left BA40 did not survive post-hoc tests.

Similar to the left handed participants, also the right handed participants showed considerable bilateral *interaction* effects in ***BA39*** (left: $F_{(2,54)} = 33.65$, $p_{(FWE)} < 0.001$; right: $F_{(2,54)} = 17.85$, $p_{(FWE)} = 0.001$). In contrast to left-handers this effect was however located more ***rostral towards the TPJ*** and showed a nearly inverse pattern. Moreover, we observed effects in the ***ventro-caudal part of BA40*** also belonging to TPJ (left: $F_{(2,54)} = 23.21$, $p_{(FWE)} < 0.001$; right: $F_{(2,54)} = 13.86$, $p_{(FWE)} = 0.007$). In the left hemisphere these effects run along the border between BA40 and BA39 and form a joint cluster together with the ***caudal part of BA22*** ($F_{(2,54)} = 21.01$, $p_{(FWE)} < 0.001$).

Table 2
Effect of trunk rotation on brain responses in a-priori defined NOI.

BA/Nuc	H	Hem	Cluster size (mm^3)	F	p(FWE)	Pos-hoc tests		MNI peak-coord. (mm)
						T(54)	Comparison	
Main Effect of Trunk Rotation (df: 2,54)								
22	RH	R	297	17.10	0.005	4.10	rL > rR	54, −16, 2
						5.65	rL > straight	
39	LH	L	675	17.34	0.004	4.59	rR > straight	−57, −61, 23
						5.73	rR > rL	
44	LH	L	594	21.57	< 0.001	6.57	rR > rL	−60, 14, 17
	RH	R	459	14.63	0.018	4.74	rL > straight	36, 2, 29
						4.52	rR > straight	
Pu/CaH	LH	L	46	12.91	0.026	4.43	rR > straight	−15, 14, −1
Interaction Trunk Rotation x Saccade Direction (df: 2,54)								
22	RH	L	918	21.01	< 0.001	4.14	ΔrR > ΔrL	−60, −55, 26
						6.18	ΔS > ΔrR	
39	LH	L	2673	26.18	< 0.001	6.23	ΔrR > ΔrL	−45, −76, 32
		R	945	11.56	0.023	n.s.		45, −67, 47
	RH	L	2916	33.65	< 0.001	8.10	ΔS > ΔrR	−57, −58, 38
		R	729	17.85	0.001	5.73	ΔS > ΔrR	54, −58, 41
40	LH	L	297	14.18	0.005	n.s.		−45, −58, 56
	RH	L	999	23.21	< 0.001	4.60	ΔrR > ΔrL	−57, −52, 35
		R	297	13.86	0.007	6.76	ΔS > ΔrR	36, −55, 62

Abbreviations: BA – Brodmann area, Nuc – nucleus, Pu – putamen, CaH – caudate head, H – Handedness, LH – left-handed, RH – right-handed, Hem – Cerebral hemisphere, L – left, R – right, FWE – family-wise error, MNI – Montreal Neurological Institute, df – degrees of freedom, rL – trunk rotation leftwards, rR – trunk rotation rightwards, S – straight trunk orientation, sL – saccade to the left, sR – saccade to the right, ΔrL - $|sL\text{-}sR|_{rL}$, ΔrR - $|sL\text{-}sR|_{rR}$, ΔS - $|sL\text{-}sR|_{S}$, n.s. – not significant.

Taken together, the commonality between the left- and right-handers is the modulation of bold responses by trunk and saccade direction in area 39 (i.e. parietal cortex): In left-handers fMRI-BOLD activity is higher within rightward rotation with the saccade towards the left hemifield target. For right-handers the opposite pattern was observed: higher activity for rightward rotation when the saccade was performed towards the right. For more details and a graphical display see Table 2 (lower part) and Fig. 6.

3.2.5. *Laterality effects*

The assessment of brain laterality effects by means of standard laterality indices revealed a clear right hemispheric response dominance over all experimental condions (LI < 0). LIs less than zero were found in 15 out of 24 values in the group of left-handed participant and in 21 out of 24 values in the group of right-handers. Left-handers showed a stronger left hemispheric brain response specifically in BA40 and, to a lesser extent also in BA44.

For further details see Table 3 and Fig. 7.

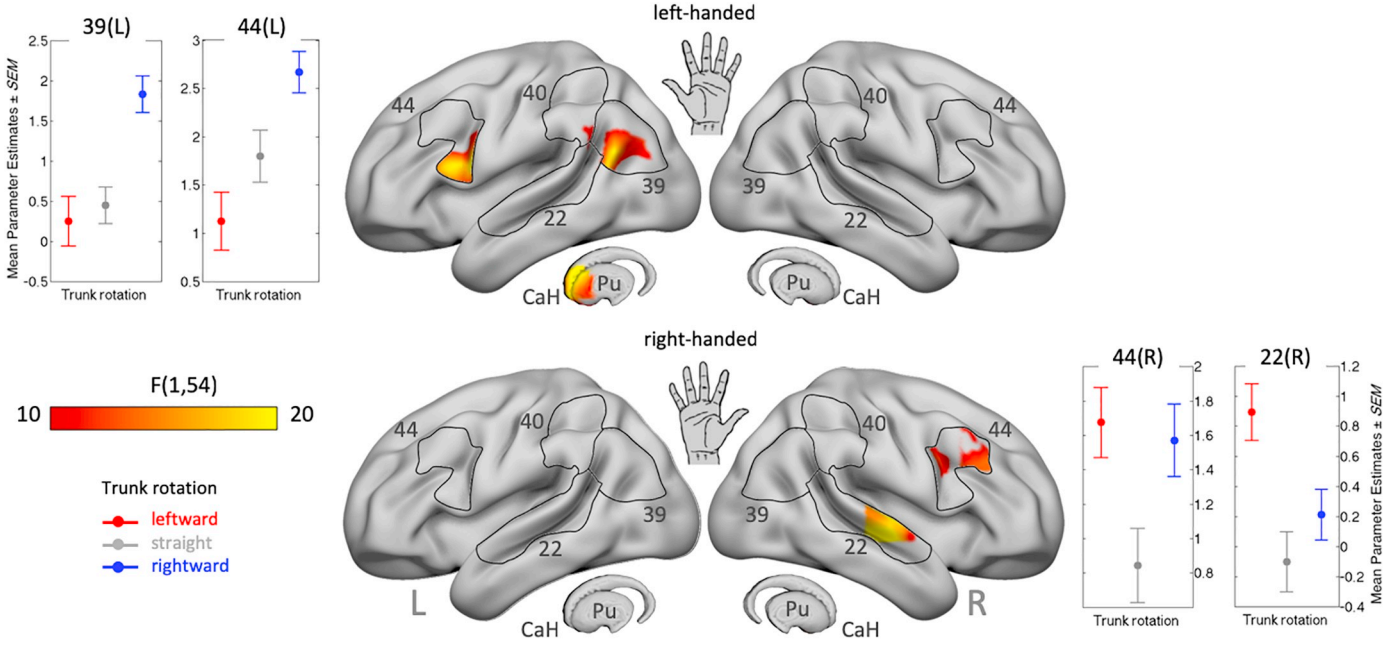

Fig. 5. Trunk rotation dependent modulation of brain responses in the a-priori defined NOI. Color-coded results of the voxel-wise F-test on the main effect of trunk rotation, restricted to voxels within the NOI as described in Fig. 2. Displayed are all effects at a statistical threshold of p < .05 (family-wise error corrected for multiple comparisons) overlaid on a slightly inflated and smoothed cortical surface of the cerebrum. Beside the brain images, mean parameter estimates of the Generalized Linear Model (GLM) extracted at peak positions are plotted for the related Brodmann areas separately (for a detailed listing see Table 3, part B). Abbreviations: L – left, R – right, Pu – putamen, CaH – caudate head. (For interpretation of the references to color in this figure legend, the reader is referred to the web version of this article.)

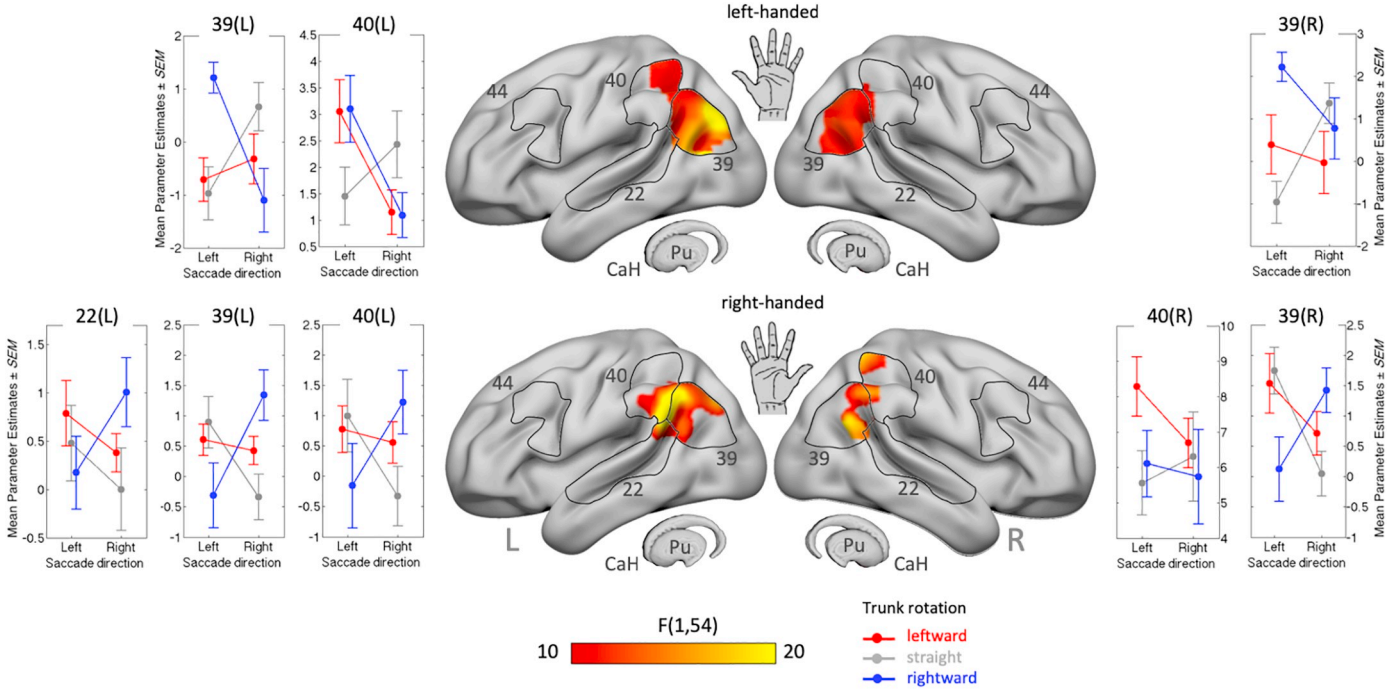

Fig. 6. Trunk rotation and saccade direction dependent modulation of brain responses in the a-priori NOI. Color-coded results of the voxel-wise F-test on the interaction between trunk rotation and saccade direction, restricted to voxels within the NOI as described in Fig. 2. Displayed are all effects at a statistical threshold of $p < .05$ (family-wise error corrected for multiple comparisons) overlaid on a slightly inflated and smoothed cortical surface of the cerebrum. Beside the brain images, mean parameter estimates of the Generalized Linear Model (GLM) extracted at peak positions are plotted for the related Brodmann areas separately (for a detailed listing see Table 3, part C). Abbreviations: L – left, R – right, Pu – putamen, CaH – caudate head. (For interpretation of the references to color in this figure legend, the reader is referred to the web version of this article.)

Table 3
Condition specific laterality (LI = {LH-RH}/{|LH| + |RH|}). Listed are medians of LIs. LIs greater than zero indicate stronger left hemispheric brain response on stimulation or a more pronounced experimental variance induction in left hemispheric brain responses and vice versa. LIs were computed according the recommendations of Seghier (2008). For a graphical display show Fig. 7.

BA	Handedness	LI						
		LL	LR	SL	SR	RL	RR	Mean LI
22	Left-handed	−0.18*	−0.17*	−0.24*	−0.18*	−0.09	−0.13*	−0.17
	Right-handed	−0.30*	−0.35*	−0.36*	−0.36*	−0.36*	−0.32*	−0.34
39	Left-handed	−0.09	−0.11	−0.01	−0.05	−0.02	−0.14	−0.07
	Right-handed	0.01	−0.14	−0.03	−0.13*	0.02	−0.07	−0.09
40	Left-handed	0.04	0.06	0.02	0.07	0.11	0.08	0.06
	Right-handed	−0.11*	−0.09*	0.00	−0.08	−0.04	−0.05	−0.06
44	Left-handed	−0.05	0.03	0.03	−0.06	0.09*	−0.03	0.00
	Right-handed	−0.09	−0.13*	−0.07	−0.16*	−0.12*	−0.17*	−0.12

Abbreviations: BA – Brodmann area, LL – leftward trunk rotation & left saccade, LR – leftward trunk rotation & right saccade, SL – straight trunk rotation & left saccade, SR – straight trunk rotation & right saccade, RL – rightward trunk rotation & left saccade, LR – rightward trunk rotation & right saccade.

* Denotes significant hemispheric differences in brain response as assessed by a two-sided Wilcoxon signed rank test ($p < .05$, uncorrected for multiple comparisons).

4. Discussion

We observed modulatory effects of three different trunk orientations (leftward, straight, rightward) on neural activation patterns during the execution of directed saccades in the context of a temporal order judgment task. Irrespective of the saccade direction fronto-temporo-parietal regions of the same hemisphere as the dominant hand are activated with highest effects in trunk positions opposite to the saccade direction. Moreover, left-handed subjects show an activation of the left putamen/caudate head during rightward trunk rotations. Depending on the performed saccade direction, trunk rotation leads to neural activation changes in BA39, close to the temporo-parietal junction (TPJ) with a right hemispheric lateralization, most pronounced in right-handers for rightward saccades.

4.1. An egocentric midline shift by trunk rotation

Up to 85% of the patients suffering from a right-hemispheric stroke show neglect symptoms (Stone et al., 1993). Neglect symptoms seem to derive from a lesion induced (perceived) deviation of the egocentric trunk midline towards the ipsilesional space (e.g. Karnath 1997, 2015). This might result in a processing mismatch between different afferent information needed to be integrated into an egocentric space representation (Pizzamiglio et al., 1997).

Interestingly, we were able to induce neglect like symptoms in healthy subjects by changing the head-on-trunk position around the vertical trunk midline in a former behavioral study (Paschke et al., 2015). We could show a selective saccadic choice bias for the hemifield ipsilateral to the direction of trunk rotation in case of spatially

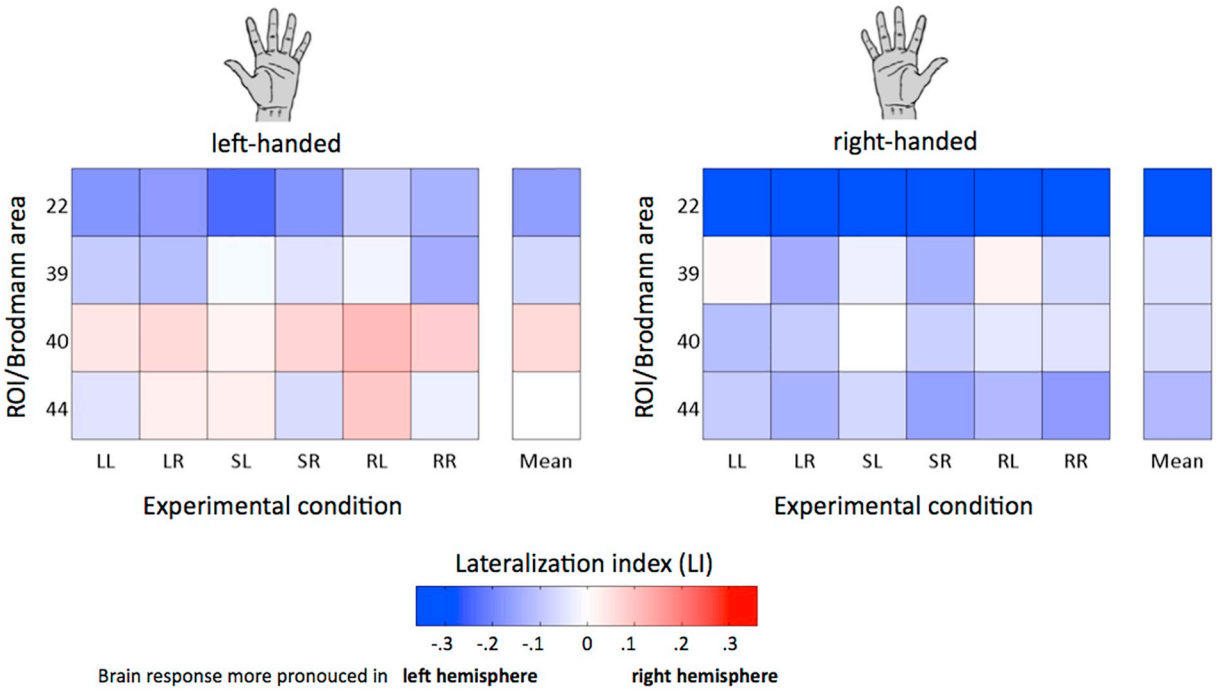

Fig. 7. Plot of lateralization indices (LI) for a-priori defined regions of interest (ROIs). Color-coded Condition x ROI matrix plot according to LIs listed in Table 3. Red colored matrix cells indicates a more pronounced brain responses in the left hemisphere, blue colored matrix cells indicates a more pronounced brain responses in the right hemisphere. Abbreviations: LH – left handers, RH – right handers, experimental condition: 1st letter – trunk orientation, 2nd letter saccade direction, LL – leftward trunk orientation | leftward saccade, LR – leftward trunk orientation | rightward saccade, SL – straight trunk orientation | leftward saccade, SR – straight trunk orientation | rightward saccade, RL – rightward trunk orientation | rightward saccade, RR – rightward trunk orientation | rightward saccade. (For interpretation of the references to color in this figure legend, the reader is referred to the web version of this article.)

congruent targets. This observation suggests an influence of the trunk position not only on time perception and processing but also on stimulus location dependent, hemifield specific (saccadic) motor responses. Hence, we concluded that a manipulation of the trunk midline affects planning/generation and integration of directed perceptually-contingent motor responses in a body-centered reference frame but not the perceptual performance per se. Although our fMRI-optimized task design was not sensitive enough to observe a trunk-rotation induced choice bias, this interpretation is supported by our current finding of saccadic speed alteration in left-handers: In particular, subjects showed a decrease of saccadic speed for left hemifield targets in rightward rotation suggesting an ipsilateral trunk-rotation induced motor delay. Rorden and colleagues reported a similar modulation of the temporal and spatial bias in the TOJ task in spatial neglect patients by changing stimulus positions relative to the subject's trunk position (Li et al., 2017). The temporal and spatial bias showed a tight association, suggesting a lesion-induced disturbance of a common spatio-temporal processing rather than of isolated perceptual processes. In addition, Roberts et al. (2012) could link spatial and temporal aspects during the TOJ task in neglect patients to distinct neural areas: spatial deficits occurred after lesions in the contralateral temporoparietal cortex (AG, SMG, STG) whereas temporal deficits were associated with lesions in the right parietal lobe and cerebellum.

In the current study we focused on the key regions associated with spatial neglect: STG (BA 22), AG and IPL (BA 39), vPCG and SMG (BA 40), pars op. IFG and pMFG (BA 44) and the basal ganglia core regions putamen, caudate nucleus, and pallidum (Chechlacz et al., 2012a; Halligan et al., 2003; Harvey and Rossit, 2012; Jacobs et al., 2012; Karnath et al., 2001; Molenbergh et al., 2012; Mort, 2003, Karnath et al., 2004; Karnath et al., 2011, Molenberghs et al., 2012). A shift of the trunk midline modulated neural activation in temporoparietal BA 44 (LH) and BA 22 (RH) as well as frontal BA 22 (LH, RH) and putamen/caudate head (LH) of the non-dominant hemisphere. Thus, the intensity of neural activity, even performing the same TOJ-task depends on the body posture. When relating the trunk rotation to the saccade direction, large effects could be observed at the junction of BA22, BA 39, and BA 40, an area referring to TPJ with right-hemispheric dominance. Interestingly, in right-handed subjects a trunk rotation towards the right hemifield mostly led to decreased activation for saccades to the left and increased activation for saccades to the right compared to a straight and leftward-oriented trunk midline. Left-handers showed a different pattern but also a clear influence of trunk orientation on saccades and neural activations. Hence, the role of the TPJ in integrating endogenous and exogenous signals to align different coordinate systems and influence motor responses is supported by our results.

TPJ (including SMG, AG, and superior temporal cortex) together with the posterior insula are discussed as human homologue to the monkey parieto-insular vestibular cortex (PIVC). In monkeys PIVC covers multimodal areas receiving information from the peripheral vestibular apparatus via thalamic regions and interacting with frontal, parietal and cingulate cortex areas (Lopez and Blanke, 2011). According to Carter and Huettel (2013), the propagation of information and its increasingly complex processing - up to social cognition - along the inferior superior axis of TPJ, starts with perceptual and attentional inputs. They concluded, that TPJ serves as a kind of nexus or hub, integrating information from several, converging multimodal processing streams. Such information integration is in turn, a requirement for successful goal directed behavior. In line with this notion, Corbetta et al. (2008) describe the right TPJ as a key region for processing behaviorally relevant stimuli.

All three aspects support the view, that the TPJ as multimodal region linking spatiotemporal information also with information of the trunk position (Bremmer et al., 2001; Brotchie et al., 2003; Mullette-Gillman et al., 2005). An egocentric midline shift by trunk rotation leads to alterations of afferent neck-proprioceptive information and a shift of the internal body-centered coordinates. Visual signals are integrated in a global, body- or egocentric reference frame to allow an

optimal space orientation. A functional interrelationship between visuomotor and proprioceptive postural signal processing is additionally underlined by illusory perception of body rotation induced by vibratory stimulation of the posterior neck muscles (Goodwin et al., 1972) and by studies showing effects of neck vibration on reaching (Biguer et al., 1988), and eye movement behavior (Fujiwara et al., 2009).

4.2. Laterality effects

We could show an important influence of handedness on trunk rotation induced effects. More precisely, we observed an ipsilateral acceleration of saccadic speed modulated by trunk orientation and individual handedness. Overall and in accordance with former behavioral experiments (Paschke et al., 2015), left-handed participants showed the strongest effects suggesting greater susceptibility to trunk manipulation. A possible explanation might be that left-handed people show greater flexibility of hand usage in daily life. Hence, a more precise and flexible integration of postural information might be of higher relevance than for right-handed people (Petit et al., 2015). This is supported by the finding that left-handers represent body space more accurately than right-handers (Hach and Schütz-Bosbach, 2014; Linkenauger et al., 2009).

Within our a priori chosen fronto-temporo-parietal network, we observed a trunk orientation dependence of brain responses with greatest effects in the hemisphere ipsilateral to the dominant hand. Accordingly, Dieterich et al. (2003) described a lateralization of vestibular cortical functions. The authors investigated cortical activation during caloric vestibular stimulation in right- and left-handers. Cortical and subcortical areas including SMG and STG responded most to stimulation of the ear ipsilateral to the hemisphere ipsilateral to the dominant hand. Thus, greatest activations were found in the right-hemisphere of right-handed subjects during caloric irrigation of the right ear and vice versa for left-handed subjects. Our findings together with the results of Dieterich et al. (2003) suggest a processing of the body orientation in the hemisphere ipsilateral to the dominant hand.

Notably, when considering trunk orientation and the direction of the saccadic response a right-hemispheric lateralization could be found most pronounced in right-handed subjects. Hence, both handedness groups showed different activation patterns. The overall smaller lateralization indices in left-handers favor theories of less hemispheric specialization and a greater requirement for interhemispheric interactions in this group (Wada et al., 2004). Further support of this hypothesis comes from the finding that on average left-handers have a larger extent of bi-hemispheric language representation (Josse et al., 2006), no hemispheric bias in face- and body-related extrastriate areas (Willems et al., 2009), and a higher density of axons in the corpus collosum than right-handers (Westerhausen et al., 2004; Witelson, 1985). Moreover, right-handers exhibit larger deactivation of the ipsilateral primary motor cortex (M1) when moving their dominant compared to their non-dominant hand, whereas left-handers show similar M1 deactivations irrespective of the moving hand (Tzourio-Mazoyer et al., 2015). The authors explain their results by a more bilateral manual cortical specialization in left-handers and the strength of transcallosal inhibition to be greater with greater manual ability asymmetry.

Nevertheless, in the current study left-handers showed also right-hemispheric dominance in temporo-parietal regions but to a smaller extent than right-handers. This is in line with findings of a weaker hemispheric lateralization in left-handers also in other cognitive domains. Recent fMRI studies on large samples of right- and left-handers support this view for language (Mazoyer et al., 2014) but also for spatial functions (Hervé et al., 2013; Petit et al., 2015). Studies applying transcranial Doppler sonography showed a predominance of left hemispheric lateralization for language for both handedness groups (95% for right-handers and 75% for left-handers, respectively, Knecht et al., 2000) and a predominance of right hemispheric lateralization for spatial memory functions (75% for both groups, Whitehouse and Bishop, 2009). Furthermore, Petit et al. (2015) applied a visually guided saccade task in a sample of 293 healthy, left- and right-handed subjects. They reported a right hemispheric dominance of areas belonging to the ventral attention network irrespective of hand preference, and a right hemispheric dominance of fronto-parietal areas belonging to the dorsal attention network (even pronounced more in left-handers compared to right-handers). Interestingly, the authors could show the strongest rightward lateralization in fronto-parietal regions of left-handers with right eye dominance underlying the importance of both laterality parameters.

5. Limitations

Due to the restrictions of MRI scanning, it was necessary to adapt the task settings to fulfill event-related fMRI-requirements. Thus, subjects were lying instead of sitting meaning that the rotation around their vertical body axis was in the horizontal instead of the vertical plane. Pizzamiglio et al. (1997) could show that neglect patients, unlike brain-damaged patients without neglect, strongly reduced their ipsilesional directional error in the supine compared to the upright position in a basic line bisection task. The authors argue that the gravitational information from the vestibular system is strongly reduced in the supine position. Moreover, instead of a rotation of 60°, in the scanner a rotation of only 45° could be realized. Additionally, the timing of the TPJ task had to be slowed down significantly to match the event-related fMRI design. This design alteration and the limited overall experimental duration resulted in inter-trial-intervals (ITIs) of up to 10 s and less trial repetitions. All of these aspects lead to a reduction in task efficacy. Moreover, it is also possible that some of our trunk-rotation related activity patterns are modulated by task effort and attention.

The observed trunk rotation associated differences in SNR (LH: left BA22; RH: left BA22, right BA22 & 44 and putamen/caudate) could lead to a different goodness of model fit and, thus, to different model sensitivities. Indeed, we found no effects of trunk rotation on brain responses in these regions, although the exact influence of SNR differences on our findings remains unclear. However, the reader should keep this problem in mind while assessing our results.

Furthermore, we found evidence for an important influence of handedness and ocular dominance on the processing of body orientation and spatial acting. Our sample included left eye dominance in three out of twelve right-handed and six out of twelve left-handed participants. Hence, the sample was too small to investigate the effect of the ocular dominance associated spatial bias. But since we knew the importance of this laterality parameter, we included it as covariate in our SPM models. A greater sample is needed to gain more insight into this interesting field of research.

6. Conclusion

We could demonstrate neural activation in fronto-temporo-parietal as well as basal ganglia (putamen/caudate head) regions to be affected by trunk orientation with greatest effects following contralateral trunk rotation in the non-dominant hemisphere suggesting gain modulatory and laterality effects. The named regions are linked to spatial neglect symptoms as known from lesion studies. Left-handed subjects showed the strongest behavioral and neural effects suggesting greater susceptibility to trunk manipulation. When considering the (saccadic) motor response in relation to the trunk orientation, TPJ appeared as a key region with a right-hemispheric lateralization. Thus, a role of the TPJ in integrating sensory, motor, and trunk position information is supported. We could underline the importance of taking individual differences in functional laterality.

Funding

This work was supported by the German Research Foundation (WI 406/1-1) (MW), and the Herman and Lilly Schilling Foundation (MW).

Acknowledgements

We thank Peter Dechent for setting the optimal MRI parameters. We thank Kirsten Emmert for help with data collection and Severin Heumüller for excellent IT-support. Additionally, we thank Ilona Pfahlert and Britta Perl for their support in MRI data acquisition and preparing the subjects.

Appendix A. Supplementary data

Supplementary data to this article can be found online at https://doi.org/10.1016/j.nicl.2019.101898.

References

Andersen, R.A., Gnadt, J.W., 1989. Posterior parietal cortex. Rev. Oculomot. Res. 3, 315–335.
Andersen, R.A., Snyder, L.H., Li, C.S., Stricanne, B., 1993. Coordinate transformations in the representation of spatial information. Current opinion in neurobiology 3 (2), 171–176.
Annett, M., 2000. Predicting combinations of left and right asymmetries. Cortex 36 (4), 485–505. https://doi.org/10.1016/S0010-9452(08)70534-3.
Arend, I., Rafal, R., Ward, R., 2008. Spatial and temporal deficits are regionally dissociable in patients with pulvinar lesions. Brain 131 (8), 2140–2152.
Ashburner, J., Friston, K.J., 2005. Neuroimage 26 (3), 839–851 Unified segmentation.
Baylis, G.C., Simon, S.L., Baylis, L.L., Rorden, C., 2002. Visual extinction with double simultaneous stimulation: what is simultaneous? Neuropsychologia 40 (7), 1027–1034.
Biguer, B., Donaldson, I.M.L., Hein, A., Jeannerod, M., 1988. Neck muscle vibration modifies the representation of visual motion and direction in man. Brain 111 (6), 1405–1424. https://doi.org/10.1093/brain/111.6.1405.
Bourassa, D.C., McManus, I.C., Bryden, M.P., 1996. Handedness and eye-dominance: a meta-analysis of their relationship. Laterality: Asymmetries of Body 1 (1), 5–34 Brain and Cognition.
Bremmer, F., Schlack, A., Shah, N.J., Zafiris, O., Kubischik, M., Hoffmann, K.-P., Fink, G.R., 2001. Polymodal motion processing in posterior parietal and premotor cortex. Neuron 29 (1), 287–296. https://doi.org/10.1016/S0896-6273(01)00198-2.
Brotchie, P.R., Andersen, R.A., Snyder, L.H., Goodman, S.J., 1995. Head position signals used by parietal neurons to encode locations of visual stimuli. Nature 375 (6528), 232.
Brotchie, P.R., Lee, M.B., Chen, D.-Y., Lourensz, M., Jackson, G., Bradley, W.G., 2003. Head position modulates activity in the human parietal eye fields. NeuroImage 18 (1), 178–184. https://doi.org/10.1006/nimg.2002.1294.
Carter, R.M., Huettel, S.A., 2013. A nexus model of the temporal–parietal junction. Trends in cognitive sciences 17 (7), 328–336.
Chechlacz, M., Rotshtein, P., Bickerton, W.L., Hansen, P.C., Deb, S., Humphreys, G.W., 2010. Separating neural correlates of allocentric and egocentric neglect: distinct cortical sites and common white matter disconnections. Cognitive Neuropsychology 27 (3), 277–303.
Chechlacz, M., Rotshtein, P., Humphreys, G.W., 2012a. Neuroanatomical dissections of unilateral visual neglect symptoms: ALE meta-analysis of lesion-symptom mapping. Front. Hum. Neurosci. 6, 230.
Chechlacz, M., Rotshtein, P., Roberts, K.L., Bickerton, W.-L., Lau, J.K.L., Humphreys, G.W., 2012b. The prognosis of allocentric and egocentric neglect: evidence from clinical scans. PLoS One 7 (11), e47821. https://doi.org/10.1371/journal.pone.0047821.
Chechlacz, M., Rotshtein, P., Hansen, P.C., Deb, S., Riddoch, M.J., Humphreys, G.W., 2013. The central role of the temporo-parietal junction and the superior longitudinal fasciculus in supporting multi-item competition: evidence from lesion-symptom mapping of extinction. Cortex 49 (2), 487–506.
Chokron, S., Dupierrix, E., Tabert, M., Bartolomeo, P., 2007. Experimental remission of unilateral spatial neglect. Neuropsychologia 45 (14), 3127–3148. https://doi.org/10.1016/j.neuropsychologia.2007.08.001.
Cohen, Y.E., Andersen, R.A., 2002. A common reference frame for movement plans in the posterior parietal cortex. Nat. Rev. Neurosci. 3 (7), 553–562. https://doi.org/10.1038/nrn873.
Colby, C.L., 1998. Action-oriented spatial reference frames in cortex. Neuron 20 (1), 15–24.
Corbetta, M., Patel, G., Shulman, G.L., 2008. The reorienting system of the human brain: from environment to theory of mind. Neuron 58 (3), 306–324.
Crawford, J.D., Henriques, D.Y., Medendorp, W.P., 2011. Three-dimensional transformations for goal-directed action. Annual review of neuroscience 34, 309–331.
Dieterich, M., Bense, S., Lutz, S., Drzezga, A., Stephan, T., Bartenstein, P., Brandt, T., 2003. Dominance for vestibular cortical function in the non-dominant hemisphere. Cereb. Cortex 13 (9), 994–1007. https://doi.org/10.1093/cercor/13.9.994.
Efron, R., 1963. The effect of handedness on the perception of simultaneity and temporal order. Brain 86 (2), 261–284.
Ferber, S., Karnath, H.O., 1999. Parietal and occipital lobe contributions to perception of straight ahead orientation. Journal of Neurology. Neurosurgery & Psychiatry 67 (5), 572–578.
Fink, G.R., Marshall, J.C., Weiss, P.H., Stephan, T., Grefkes, C., Shah, N.J., Dieterich, M., 2003. Performing allocentric visuospatial judgments with induced distortion of the egocentric reference frame: an fMRI study with clinical implications. NeuroImage 20 (3), 1505–1517. https://doi.org/10.1016/j.neuroimage.2003.07.006.
Fruhmann-Berger, M., Karnath, H.O., 2005. Spontaneous eye and head position in patients with spatial neglect. Journal of neurology 252 (10), 1194–1200.
Fujiwara, K., Kunita, K., Furune, N., 2009. Effect of vibration stimulation to neck extensor muscles on reaction time in various saccadic eye movements. Int. J. Neurosci. 119 (10), 1925–1940. https://doi.org/10.1080/00207450802333912.
Geffen, G., Rosa, V., Luciano, M., 2000. Effects of preferred hand and sex on the perception of tactile simultaneity. Journal of Clinical and Experimental Neuropsychology 22 (2), 219–231.
Goodwin, G.M., McCloskey, D.I., Matthews, P.B., 1972. Proprioceptive illusions induced by muscle vibration: contribution by muscle spindles to perception? Science (New York, N.Y.) 175 (4028), 1382–1384.
Hach, S., Schütz-Bosbach, S., 2014. In (or outside of) your neck of the woods: laterality in spatial body representation. Front. Psychol. 5. https://doi.org/10.3389/fpsyg.2014.00123.
Halligan, P.W., Fink, G.R., Marshall, J.C., Vallar, G., 2003. Spatial cognition: evidence from visual neglect. Trends in cognitive sciences 7 (3), 125–133.
Harvey, M., Rossit, S., 2012. Visuospatial neglect in action. Neuropsychologia 50 (6), 1018–1028.
Hervé, P.-Y., Zago, L., Petit, L., Mazoyer, B., Tzourio-Mazoyer, N., 2013. Revisiting human hemispheric specialization with neuroimaging. Trends Cogn. Sci. 17 (2), 69–80. https://doi.org/10.1016/j.tics.2012.12.004.
Hornak, J., 1992. Ocular exploration in the dark by patients with visual neglect. Neuropsychologia 30 (6), 547–552.
Jacobs, S., Brozzoli, C., Farnè, A., 2012. Neglect: a multisensory deficit? Neuropsychologia 50 (6), 1029–1044.
Jamadar, S.D., Fielding, J., Egan, G.F., 2013. Quantitative meta-analysis of fMRI and PET studies reveals consistent activation in fronto-striatal-parietal regions and cerebellum during antisaccades and prosaccades. Front. Psychol. 4. https://doi.org/10.3389/fpsyg.2013.00749.
Johannsen, L., Ackermann, H., Karnath, H.-O., 2003. Lasting amelioration of spatial neglect by treatment with neck muscle vibration even without concurrent training. J. Rehabil. Med. 35 (6), 249–253.
Josse, G., Hervé, P.-Y., Crivello, F., Mazoyer, B., Tzourio-Mazoyer, N., 2006. Hemispheric specialization for language: brain volume matters. Brain Res. 1068 (1), 184–193. https://doi.org/10.1016/j.brainres.2005.11.037.
Karnath, H.O., 1994. Subjective body orientation in neglect and the interactive contribution of neck muscle proprioception and vestibular stimulation. Brain 117 (5), 1001–1012.
Karnath, H.O., 1997. Spatial orientation and the representation of space with parietal lobe lesions. Philosophical Transactions of the Royal Society of London. Series B: Biological Sciences 352 (1360), 1411–1419.
Karnath, H.O., 2015. Spatial attention systems in spatial neglect. Neuropsychologia 75, 61–73.
Karnath, H.-O., Rorden, C., 2012. The anatomy of spatial neglect. Neuropsychologia 50 (6), 1010–1017. https://doi.org/10.1016/j.neuropsychologia.2011.06.027.
Karnath, H.-O., Schenkel, P., Fischer, B., 1991. Trunk orientation as the determining factor of the 'contralateral'deficit in the neglect syndrome and as the physical anchor of the internal representation of body orientation in space. Brain 114 (4), 1997–2014.
Karnath, H.-O., Christ, K., Hartje, W., 1993. Decrease of contralateral neglect by neck muscle vibration and spatial orientation of trunk midline. Brain 116 (2), 383–396.
Karnath, H.-O., Fetter, M., Dichgans, J., 1996. Ocular exploration of space as a function of neck proprioceptive and vestibular input—observations in normal subjects and patients with spatial neglect after parietal lesions. Exp. Brain Res. 109 (2), 333–342.
Karnath, H.O., Ferber, S., Himmelbach, M., 2001. Spatial awareness is a function of the temporal not the posterior parietal lobe. Nature 411 (6840), 950.
Karnath, H.-O., Berger, Monika Fruhmann, Küker, Wilhelm, Rorden, Chris, 2004. The anatomy of spatial neglect based on Voxelwise statistical analysis: a study of 140 patients. Cereb. Cortex 14 (10), 1164–1172. https://doi.org/10.1093/cercor/bhh076.
Karnath, H.-O., Rennig, J., Johannsen, L., Rorden, C., 2011. The anatomy underlying acute versus chronic spatial neglect: a longitudinal study. Brain 134 (3), 903–912. https://doi.org/10.1093/brain/awq355.
Klein, S.A., 2001. Measuring, estimating, and understanding the psychometric function: A commentary. Perception & psychophysics 63 (8), 1421–1455.
Kleinman, J.T., Newhart, M., Davis, C., Heidler-Gary, J., Gottesman, R.F., Hillis, A.E., 2007. Right hemispatial neglect: frequency and characterization following acute left hemisphere stroke. Brain Cogn. 64 (1), 50–59. https://doi.org/10.1016/j.bandc.2006.10.005.
Knecht, S., Dräger, B., Deppe, M., Bobe, L., Lohmann, H., Flöel, A., ... Henningsen, H., 2000. Handedness and hemispheric language dominance in healthy humans. Brain J. Neurol. 123 (Pt 12), 2512–2518.
Lehky, S.R., Tanaka, K., 2016. Neural representation for object recognition in inferotemporal cortex. Curr. Opin. Neurobiol. 37, 23–35. https://doi.org/10.1016/j.conb.2015.12.001.
Li, D., Karnath, H.-O., Rorden, C., 2014. Egocentric representations of space co-exist with allocentric representations: evidence from spatial neglect. Cortex 58, 161–169. https://doi.org/10.1016/j.cortex.2014.06.012.

Li, D., Rorden, C., Karnath, H.O., 2017. “Nonspatial” attentional deficits interact with spatial position in neglect. Journal of cognitive neuroscience 29 (5), 911–918.
Linkenauger, S.A., Witt, J.K., Bakdash, J.Z., Stefanucci, J.K., Proffitt, D.R., 2009. Asymmetrical body perception: a possible role for neural body representations. Psychol. Sci. 20 (11), 1373–1380. https://doi.org/10.1111/j.1467-9280.2009.02447.x.
Lopez, C., Blanke, O., 2011. The thalamocortical vestibular system in animals and humans. Brain research reviews 67 (1-2), 119–146.
Måns Magnusson, Rorsman, Ba, I., 1999. Reduction of visuo-spatial neglect with vestibular galvanic stimulation. Scand. J. Rehabil. Med. 31 (2), 117–124. https://doi.org/10.1080/003655099444632.
Mazoyer, B., Zago, L., Jobard, G., Crivello, F., Joliot, M., Perchey, G., ... Tzourio-Mazoyer, N., 2014. Gaussian mixture modeling of hemispheric lateralization for language in a large sample of healthy individuals balanced for handedness. PLoS One 9 (6), e101165. https://doi.org/10.1371/journal.pone.0101165.
McManus, I.C., 1999. Eye-dominance, writing hand, and throwing hand. Laterality: Asymmetries of Body, Brain and Cognition 4 (2), 173–192. https://doi.org/10.1080/713754334.
Molenberghs, P., Sale, M.V., Mattingley, J.B., 2012. Is there a critical lesion site for unilateral spatial neglect? A meta-analysis using activation likelihood estimation. Front. Hum. Neurosci. 6. https://doi.org/10.3389/fnhum.2012.00078.
Moon, S., Lee, B., Na, D., 2006. Therapeutic effects of caloric stimulation and optokinetic stimulation on Hemispatial neglect. J. Clin. Neurol. 2 (1), 12. https://doi.org/10.3988/jcn.2006.2.1.12.
Mort, D.J., Malhotra, P., Mannan, S.K., Rorden, C., Pambakian, A., Kennard, C., Husain, M., 2003. The anatomy of visual neglect. Brain 126 (9), 1986–1997.
Mullette-Gillman, O.A., Cohen, Y.E., Groh, J.M., 2005. Eye-centered, head-centered, and complex coding of visual and auditory targets in the intraparietal sulcus. J. Neurophysiol. 94 (4), 2331–2352. https://doi.org/10.1152/jn.00021.2005.
Oldfield, R.C., 1971. The assessment and analysis of handedness: the Edinburgh inventory. Neuropsychologia 9 (1), 97–113.
Paschke, K., Kagan, I., Wüstenberg, T., Bähr, M., Wilke, M., 2015. Trunk rotation affects temporal order judgments with direct saccades: influence of handedness. Neuropsychologia 79, 123–137. https://doi.org/10.1016/j.neuropsychologia.2015.10.031.
Pauli, W.M., Nili, A.N., Tyszka, J.M., 2018. A high-resolution probabilistic in vivo atlas of human subcortical brain nuclei. Sci. Data 5, 180063.
Petit, L., Zago, L., Mellet, E., Jobard, G., Crivello, F., Joliot, M., ... Tzourio-Mazoyer, N., 2015. Strong rightward lateralization of the dorsal attentional network in left-handers with right sighting-eye: an evolutionary advantage: spatial attention, handedness, and eyedness. Hum. Brain Mapp. 36 (3), 1151–1164. https://doi.org/10.1002/hbm.22693.
Pierrot-Deseilligny, C., Milea, D., Müri, R.M., 2004. Eye movement control by the cerebral cortex. Curr. Opin. Neurol. 17 (1), 17–25.
Pizzamiglio, L., Vallar, G., Doricchi, F., 1997. Gravitational inputs modulate visuospatial neglect. Exp. Brain Res. 117 (2), 341–345. https://doi.org/10.1007/s002210050227.
Ro, T., Rorden, C., Driver, J., Rafal, R., 2001. Ipsilesional biases in saccades but not perception after lesions of the human inferior parietal lobule. J. Cogn. Neurosci. 13 (7), 920–929. https://doi.org/10.1162/089892901753165836.
Roberts, K.L., Lau, J.K., Chechlacz, M., Humphreys, G.W., 2012. Spatial and temporal attention deficits following brain injury: a neuroanatomical decomposition of the temporal order judgement task. Cognitive neuropsychology 29 (4), 300–324.
Rode, G., Perenin, M.-T., 1994. Temporary remission of representational hemineglect through vestibular stimulation. Neuroreport 5 (8), 869–872.
Rorden, C., Mattingley, J.B., Karnath, H.O., Driver, J., 1997. Visual extinction and prior entry: Impaired perception of temporal order with intact motion perception after unilateral parietal damage. Neuropsychologia 35 (4), 421–433.
Schindler, I., 2002. Neck muscle vibration induces lasting recovery in spatial neglect. J. Neurol. Neurosurg. Psychiatry 73 (4), 412–419. https://doi.org/10.1136/jnnp.73.4.412.
Schindler, I., Kerkhoff, G., 1997. Head and trunk orientation modulate visual neglect. Neuroreport 8 (12), 2681–2685.
Seghier, M.L., 2008. Laterality index in functional MRI: methodological issues. Magnetic resonance imaging 26 (5), 594–601.
Sinnett, S., Juncadella, M., Rafal, R., Azañón, E., Soto-Faraco, S., 2007. A dissociation between visual and auditory hemi-inattention: evidence from temporal order judgements. Neuropsychologia 45 (3), 552–560. https://doi.org/10.1016/j.neuropsychologia.2006.03.006.
Spence, C., Parise, C., 2010. Prior-entry: a review. Conscious. Cogn. 19 (1), 364–379. https://doi.org/10.1016/j.concog.2009.12.001.
Stone, S.P., Halligan, P.W., Greenwood, R.J., 1993. The incidence of neglect phenomena and related disorders in patients with an acute right or left hemisphere stroke. Age Ageing 22 (1), 46–52. https://doi.org/10.1093/ageing/22.1.46.
Suchan, J., Rorden, C., Karnath, H.-O., 2012. Neglect severity after left and right brain damage. Neuropsychologia 50 (6), 1136–1141. https://doi.org/10.1016/j.neuropsychologia.2011.12.018.
Tzourio-Mazoyer, N., Petit, L., Zago, L., Crivello, F., Vinuesa, N., Joliot, M., ... Mazoyer, B., 2015. Between-hand difference in ipsilateral deactivation is associated with hand lateralization: fMRI mapping of 284 volunteers balanced for handedness. Front. Hum. Neurosci. 9, 5.
Ventre, J., Flandrin, J.M., Jeannerod, M., 1984. In search for the egocentric reference. A neurophysiological hypothesis. Neuropsychologia 22 (6), 797–806.
Wada, M., Yamamoto, S., Kitazawa, S., 2004. Effects of handedness on tactile temporal order judgment. Neuropsychologia 42 (14), 1887–1895. https://doi.org/10.1016/j.neuropsychologia.2004.05.009.
Westerhausen, R., Kreuder, F., Sequeira, S.D.S., Walter, C., Woerner, W., Wittling, R.A., Wittling, W., 2004. Effects of handedness and gender on macro- and microstructure of the corpus callosum and its subregions: a combined high-resolution and diffusion-tensor MRI study. Cogn. Brain Res. 21 (3), 418–426. https://doi.org/10.1016/j.cogbrainres.2004.07.002.
Whitehouse, A.J.O., Bishop, D.V.M., 2009. Hemispheric division of function is the result of independent probabilistic biases. Neuropsychologia 47 (8–9), 1938–1943. https://doi.org/10.1016/j.neuropsychologia.2009.03.005.
Wichmann, F.A., Hill, N.J., 2001. The psychometric function: I. Fitting, sampling, and goodness of fit. Perception & psychophysics 63 (8), 1293–1313.
Wilkinson, D., Zubko, O., Sakel, M., Coulton, S., Higgins, T., Pullicino, P., 2014. Galvanic vestibular stimulation in hemi-spatial neglect. Front. Integr. Neurosci. 8. https://doi.org/10.3389/fnint.2014.00004.
Willems, R.M., Peelen, M.V., Hagoort, P., 2009. Cerebral lateralization of face-selective and body-selective visual areas depends on handedness. Cereb. Cortex 20 (7), 1719–1725.
Witelson, S.F., 1985. The brain connection: the corpus callosum is larger in left-handers. Science (New York, N.Y.) 229 (4714), 665–668.
Woo, S.-H., Kim, K.-H., Lee, K.-M., 2009. The role of the right posterior parietal cortex in temporal order judgment. Brain Cogn. 69 (2), 337–343. https://doi.org/10.1016/j.bandc.2008.08.006.